Structural Optimization with Dynamic Behavior Constraints

W. C. Mills-Curran*
Sandia National Laboratories, Albuquerque, New Mexico

and

L. A. Schmit†
The University of California, Los Angeles, California

The minimum weight optimum design of damped linear elastic structural systems is addressed. The structures are subjected to periodic loading with behavior constraints on maximum deflections and side constraints on design variables. Attention is focused on the two major impediments to an optimal solution: 1) the time-dependent nature of the behavior constraints, and 2) the severe nonconvexity of the design space which is caused by the dynamic response constraints. A solution method based on upper bound approximations for the behavior constraints and an innovative mathematical programming scheme for seeking the optimal frequency subspace is set forth. Numerical results for two test problems illustrate the effectiveness of the method reported.

Nomenclature

$[A]$ = structural load matrix
A = cross-sectional area
B = set of constrained nodal responses, base dimension of element cross section
$\tilde{\boldsymbol{B}}$ = vector of sets containing nodal responses involved in stress constraints
$[e]$ = sign function matrix
g = structural damping parameter
H = height dimension of element cross section
$[I]$ = identity matrix
i = $\sqrt{-1}$
I_{yy}, I_{zz} = moment of inertia about the Y and Z axis, respectively
$[J]$ = Jacobian matrix of first-order derivatives
J = number of structural degrees of freedom, polar moment of inertia about X axis (thin-wall assumption)
$[K]$ = structural stiffness matrix
$[M]$ = structural mass matrix
$\tilde{M}$ = structural mass
P = number of load frequencies
R = number of retained structural modes ($R \leq J$)
t = time
t_h, t_b = wall thickness of element cross section
$\boldsymbol{U}$ = nodal response vector
$\boldsymbol{U}_{\text{mad}}$ = maximum absolute displacement vector
$\boldsymbol{X}$ = section property vector
$\boldsymbol{Y}$ = cross-section dimension (CSD) vector
$\boldsymbol{\alpha}$ = design variable vector
η = constraint padding parameter
$\boldsymbol{\lambda}$ = structural eigenvalue vector ($\omega_i^2 = \lambda_i$)
$[\Phi]$ = modal matrix of mass-normalized eigenvectors
$[\psi]$ = phase shift matrix
$\boldsymbol{\Omega}$ = load function frequency vector
$\boldsymbol{\omega}$ = natural frequency vector

Presented as Paper 83-0936 at the AIAA/ASME/ASCE/AHS 24th Structures, Structural Dynamics and Materials Conference, Lake Tahoe, Nev., May 2-4, 1983; received June 7, 1983; revision received March 2, 1984.

*Staff Member. Member AIAA.
†Professor of Engineering & Applied Science. Associate Fellow AIAA.

I. Background

THE problem of dynamic response has been a topic of continued interest in the field of structural optimization. Excluding papers dealing with natural frequency as the only dynamic constraint, several references remain that deal with the response problem (see Refs. 1-12). Although several of these works incorporate a periodic loading function, only a few have discussed the severely nonconvex nature of the problem.

In Ref. 1, Cassis subjected a one-bay frame structure to a one-half period duration sine wave loading and observed that a mapping of the two-dimensional design space would exhibit a disjoint feasible region for some combinations of displacement constraints and loadings. Although the loading was not periodic and, therefore, resonance could not occur, Cassis pointed out that the disjoint feasible region was due to the sinusoidal contributions to the response of the structure.

In 1976, Johnson[2] mapped the two-dimensional design space for the steady-state response of a periodically loaded structure. This mapping (Fig. 1) clearly shows that the feasible regions are separated by a locus of points (indicated by the dotted line) representing designs where a natural frequency of the structure equals the frequency of the loading function. The infeasible region on either side of this locus is due to a displacement constraint. It is then clear that the cause of the disjoint feasible regions in this class of design problems is the resonance of the natural frequencies with the loading frequencies.

II. Problem Statement

The general problem of optimizing a periodically loaded structure is stated in its simplest form as follows. Find the design vector ($\boldsymbol{\alpha}$) that minimizes structural mass [$\tilde{M}(\boldsymbol{\alpha})$] subject to displacement constraints ($\boldsymbol{U}^u$) on the steady-state response, and side constraints ($\boldsymbol{\alpha}^l$, $\boldsymbol{\alpha}^u$) on the design vector.

Mathematically, this is written

$$\min_{\boldsymbol{\alpha}} \tilde{M}(\boldsymbol{\alpha}) \tag{1}$$

subject to

$$U_b(\boldsymbol{\alpha}, t) \leq U_b^u, \qquad b \in B, \qquad t \geq 0 \tag{2}$$

$$\boldsymbol{\alpha}^l \leq \boldsymbol{\alpha} \leq \boldsymbol{\alpha}^u \tag{3}$$

where B is the set of constrained nodal responses and $\boldsymbol{U}(\boldsymbol{\alpha}, t)$

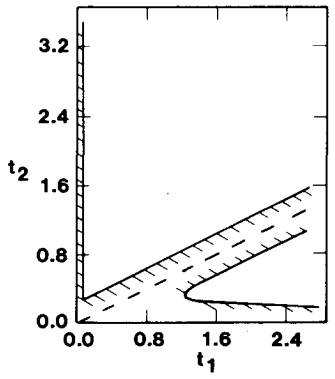

Fig. 1 Disjoint feasible region.[2]

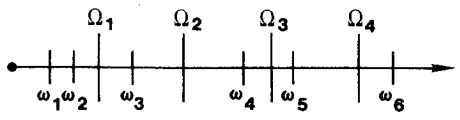

Fig. 2 Frequency number line.

is the steady-state solution to the dynamic equilibrium equations

$$\sum_{j=1}^{J}\left[M_{lj}U_j+(1+ig)K_{lj}U_j\right]=\sum_{p=1}^{P}A_{lp}\sin(\Omega_p t)$$

$$l=1,\ldots,J \quad (4)$$

where M_{lj}, K_{lj}, and A_{lp} are elements of mass, stiffness, and loading matrices, respectively, and g is the structural damping parameter for J degrees of freedom and P loading frequencies.

Disjoint Feasible Regions

Figure 2 uses a number line to show the ordering of the natural frequencies ω relative to the loading frequencies Ω for a hypothetical problem with six natural frequencies and four loading frequencies. A resonant design would be depicted by a natural frequency occupying the same location on the number line as a loading frequency. A different disjoint region, or frequency subspace, is encountered any time a natural frequency crosses over a loading frequency.

In general, a structure modeled by R modes and P loading frequencies will have $(P+1)^R$ frequency subspaces. The number line of Fig. 2 then represents a design problem with $(4+1)^6=15{,}625$ frequency subspaces, each containing a potentially feasible region.

It is certain that resonance condition designs for undamped structures will be infeasible, so that the resonant designs form a barrier which prevents a feasible design in one frequency subspace from proceeding to a superior design in a neighboring subspace. These barriers cause the design space to be disjoint as in Fig. 1. Structures which incorporate damping may not be infeasible at resonant design points, but the increased response encountered at these designs will cause the design space to be severely nonconvex rather than strictly disjoint.

It should be noted that some frequency subspaces may not contain feasible designs, due to the restrictions imposed by the constraints in the problem statement.

Time Parametric Constraint

The time parametric constraint of Eq. (2) has proved to be an expensive constraint to evaluate. For the steady-state response case treated herein, the time at which the maximum response occurs will be difficult to determine due to the interaction of the modes of the structure. This places a computational burden on time parametric constraint evaluation techniques.

The difficulties presented by the severe nonconvexities of the design space and by the time parametric constraint functions, both described above, are the main obstacles to generating a method for optimum design of structural systems involving dynamic response constraints. Methods for overcoming these difficulties are outlined in the following sections.

III. Solution Method

Time Parametric Constraint Simplification

The steady-state solution to Eq. (4) is written

$$U_b(\alpha,t)=\sum_{i=1}^{R}\sum_{p=1}^{P}\left[\Phi_{bi}\sum_{l=1}^{J}\Phi_{li}A_{lp}\sin(\Omega_p t-\psi_{ip})\div m_i\sqrt{\left(\omega_i^2-\Omega_p^2\right)^2+g^2\omega_i^4}\right] \quad (5a)$$

$$\psi_{ip}=\tan^{-1}\left[g\omega_i^2/\left(\omega_i^2-\Omega_p^2\right)\right] \quad (5b)$$

where Φ_{li} is an element of the modal matrix, m_i an element of the modal mass matrix, and R the number of retained modes.

For lightly damped structures ($0.01<g<0.04$), ψ_{ip} [Eq. (5b)] is nearly a step function, differing from a step function only near the resonance condition. Assuming that displacement constraints will prevent the design from closely approaching the resonance condition, the following approximation is made.

$$\sin(\Omega_p t-\psi_{ip})=e_{ip}\sin(\Omega_p t) \quad (6a)$$

where

$$e_{ip}=\begin{cases}1 & \omega_i>\Omega_p\\ -1 & \omega_i<\Omega_p\end{cases} \quad (6b)$$

Substituting Eqs. (6) into Eqs. (5) and reordering, $U_b(\alpha,t)$ is written

$$U_b(\alpha,t)=\sum_{p=1}^{P}\sin(\Omega_p t)\times\left\{\sum_{i=1}^{R}\left[\Phi_{bi}\sum_{l=1}^{J}\Phi_{li}A_{lp}e_{ip}\Big/m_i\sqrt{\left(\omega_i^2-\Omega_p^2\right)^2+g^2\omega_i^4}\right]\right\} \quad (7)$$

Simplifying, let

$$\gamma_{bp}=\sum_{i=1}^{R}\left[\Phi_{bi}\sum_{l=1}^{J}\Phi_{li}A_{lp}e_{ip}\Big/m_i\sqrt{\left(\omega_i^2-\Omega_p^2\right)^2+g^2\omega_i^4}\right] \quad (8)$$

so that

$$U_b(\alpha,t)=\sum_{p=1}^{P}\gamma_{bp}\sin(\Omega_p t) \quad (9)$$

Now, the constraint of Eq. (2) is rewritten

$$U_b(\alpha,t)\le U_b^u, \qquad b\in B, \qquad t\ge 0 \quad (10)$$

A substitute form for these constraints can be expressed as

$$\max_{t\ge 0}U_b(\alpha,t)\le U_b^u, \qquad b\in B \quad (11)$$

Substituting from Eq. (9),

$$\max_{t\geq 0} \sum_{p=1}^{P} \gamma_{bp} \sin(\Omega_p t) \leq U_b^u, \qquad b \in B \tag{12}$$

Assuming that the "worst-case" combination of the sinusoids of Eq. (12) will eventually occur, that equation is rewritten

$$\sum_{p=1}^{P} |\gamma_{bp}| \leq U_b^u, \qquad b \in B \tag{13}$$

which expresses maximum absolute displacement (U_{mad}) upper bounds as a simplified substitute for the time parametric constraints. The constraints are finally written as

$$U_{\text{mad}_b}(\alpha) = \sum_{p=1}^{P} \left| \sum_{i=1}^{R} \left[\Phi_{bi} \sum_{l=1}^{J} \Phi_{li} A_{lp} e_{ip} \div m_i \sqrt{\left(\omega_i^2 - \Omega_p^2\right)^2 + g^2 \omega_i^4} \right] \right| \leq U_b^u, \qquad b \in B \tag{14}$$

It is seen that the worst-case assumption is a conservative approximation that provides a simplified function [Eq. (14)] to use for constraint evaluation and gradient calculations (with respect to design variables).

In practice, Eq. (14) is evaluated by treating $U_{\text{mad}}(\alpha)$ as a nonlinear function of the eigenvalues and eigenvectors $\lambda, [\Phi]$ which are in turn approximated as linear functions of the design vector α. These linear approximations are updated as a series of approximate problems are solved. As a result, the essential nonlinearities apparent in Eq. (14) are retained, but the operational constraints become explicit functions of the design variables.

Dynamic stress constraints have not been included in the problem statement of Sec. II nor in the numerical examples of Sec. IV. However, a simple extension of the above development will allow the derivation of maximum absolute stress constraints, provided the stress can be expressed as a linear combination of nodal responses (see Ref. 17 or 21). It should be noted that extension of the upper bound approximation to combined stress failure criteria involving nonlinear functions of nodal responses (e.g., Von Mises equivalent stress) poses difficulties that are not addressed here.

Disjoint Design Space Optimization Method

Because the disjoint feature of the design space is an essential characteristic of the problem studied here, no method that avoids the inherent combinatorial nature of the interplay between the loading and natural frequencies has been found. Accepting this leads to a search that seeks to locate the design in the optimal frequency subspace by comparing local optima for all of the subspaces and then selecting the best feasible design. This approach unfortunately carries an unacceptable price, since the number of subspaces is quite large, specifically $(P+1)^R$ for P loading frequencies and R natural frequencies. A local optimum must be found for every frequency subspace that contains a feasible design.

A more limited search is then suggested which is more practical to execute, but unfortunately cannot guarantee that the globally optimal frequency subspace will be found.

This limited search pattern allows a single natural frequency to cross one forcing function frequency at a time. In this case, there are $2R$ contiguous frequency subspaces to be examined from the current frequency subspace.

It should be noted that no theoretical barrier forces the selection of a limited search, but rather that available computer resources dictate the use of a less exhaustive search. For this work, the contiguous frequency subspace search is selected.

Because the large magnitude response at near-resonant designs usually prevents currently available optimization techniques from exploring neighboring frequency subspaces, an innovative strategy has been developed to probe these neighboring subspaces. The method set forth here is most easily explained by the use of flowcharts (Figs. 3 and 4). Figure 3 shows the entire flow without detail and indicates that three subproblems are solved, labeled stages I, II, and III. The stage I problem is written

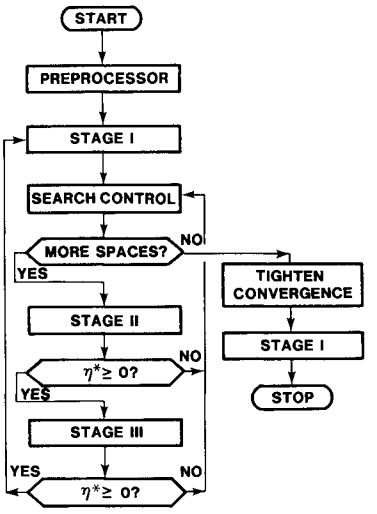

Fig. 3 Solution method flowchart.

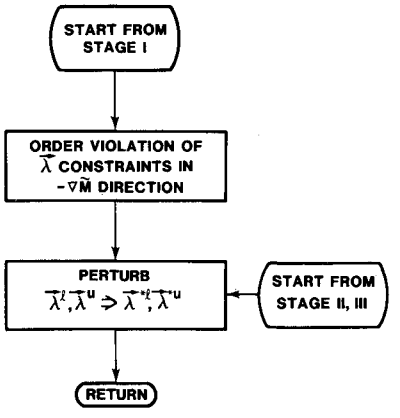

Fig. 4 Search control block.

$$\min_{\alpha} \tilde{M}(\alpha) \rightarrow \tilde{M}^* \tag{15a}$$

subject to

$$\alpha^l \leq \alpha \leq \alpha^u \tag{15b}$$

$$\lambda^l < \lambda < \lambda^u \tag{15c}$$

$$U_{\text{mad}_b} < U_b^u, \qquad b \in B \tag{15d}$$

Note that Eq. (15) is similar to Eqs. (1–3), except that Eq. (15c) has been added to insure that the design stays in the current frequency subspace. The eigenvalue limits, λ^l and λ^u, are then the boundaries of the current subspace. The solution to Eq. (15) produces the local optimal mass $\tilde{M}^*$.

When entering from the stage I problem solution, the search control block of Fig. 4 orders the neighboring frequency subspaces according to reduction of the structural mass. The frequency subspace defining eigenvalue constraints are written as a function of the design vector α and linearized about some design α_0.

$$g_i(\alpha) \cong g_i(\alpha_0) + \nabla g_i^T \Delta\alpha \qquad i = i, \ldots, 2R \tag{16}$$

When used for generating a frequency subspace search strategy, $\Delta\alpha$ is taken to be in the direction of steepest descent with a move distance of β_i:

$$\Delta\alpha = -\beta_i \nabla\tilde{M} \tag{17}$$

To find the distance to the constraint boundary for the ith constraint $g_i(\alpha) = 0$, Eq. (17) is substituted in Eq. (16) which is set to zero as follows:

$$g_i(\alpha) = 0 = g_i(\alpha_0) - \beta_i \nabla g_i^T \nabla\tilde{M} \tag{18}$$

Equation (18) is then solved for the β_i:

$$\beta_i = g_i(\alpha_0) / \nabla g_i^T \nabla\tilde{M} \tag{19}$$

The β's are separated into two groups by sign, and the members of each group are ordered according to the magnitude of their absolute value. The subspaces are then probed in order as follows: first, those associated with ascending positive values of β_i, and second, those associated with decreasing negative values of β_i. The search control block then uses this ordering scheme to vary the eigenvalue constraints λ^l, λ^u of stage I so that they represent the values that define a neighboring frequency subspace, $\lambda^{*l}, \lambda^{*u}$.

If the list of contiguous frequency subspaces is not exhausted, the stage II problem is encountered next and is written

$$\max_{\alpha,\eta} \eta \rightarrow \eta^* \tag{20a}$$

subject to

$$\alpha^l \le \alpha \le \alpha^u \tag{20b}$$

$$\lambda^{*l} + \eta \le \lambda \le \lambda^{*u} - \eta \tag{20c}$$

$$\tilde{M}(\alpha) \le \tilde{M}^* \tag{20d}$$

Note that the displacement constraints are excluded so that the resonance peak barriers are avoided. The use of the parameter η (initially negative) insures a feasible problem statement by providing a "padding" for the subspace-defining eigenvalue constraint. If the stage II problem converges with a positive value for η^*, then the design has moved to the new frequency subspace with no increase in structural mass ($\tilde{M}$) or violation of the design variable side constraints. A negative value for η indicates that this neighboring subspace does not include an improved feasible design over the stage I design.

Finally, the stage III problem is written

$$\max_{\alpha,\eta} \eta \rightarrow \eta^* \tag{21a}$$

subject to

$$\alpha^l \le \alpha \le \alpha^u \tag{21b}$$

$$\lambda^{*l} \le \lambda \le \lambda^{*u} \tag{21c}$$

$$U_{\text{mad}_b} + \eta \le U_b^u, \qquad b \in B \tag{21d}$$

$$\tilde{M}(\alpha) \le \tilde{M}^* \tag{21e}$$

The stage III problem reintroduces the displacement constraint, and again insures problem feasibility by use of the parameter η (initially negative). As in stage II, a negative η^* will eliminate this subspace from further consideration, while a positive η^* will cause stage I to be restarted within the new frequency subspace.

Note from Fig. 3 that a negative η^* from either stage II or III will cause a transfer to the search control block for selection of a new trial subspace. If no untried subspaces remain, the convergence requirements are tightened for a last pass through the stage I problem.

It should be understood that the method of solution of the stage I, II, and III problems is by solution of a series of simplified approximate problems similar to the ACCESS codes.[13-15]

The interaction of the three problem stages describes a lower bound/upper bound process similar in spirit to that used in Ref. 16. Each solution to the stage I problem defines an upper bound on the globally optimal solution. The stage II problem then seeks a neighboring frequency subspace that will reduce this upper bound by solving a problem which includes the stage I mass as an upper bound, but ignores the dynamic displacement constraints. Because the stage II problem con-

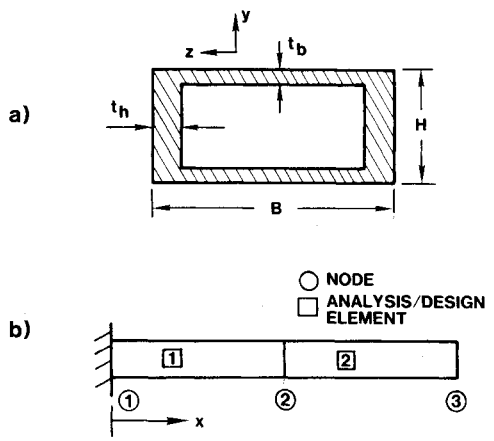

Fig. 5 Two degree of freedom shaft (example 1).

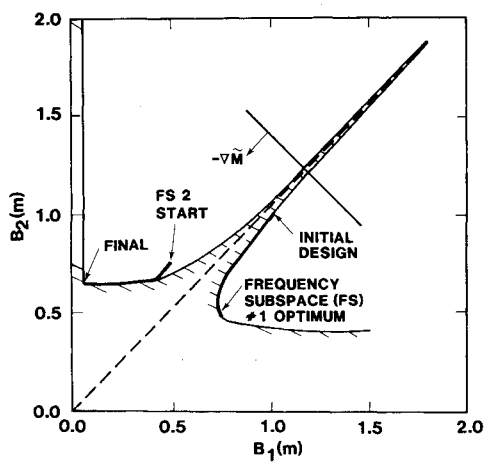

Fig. 6 Two degree of freedom shaft design space (example 1).

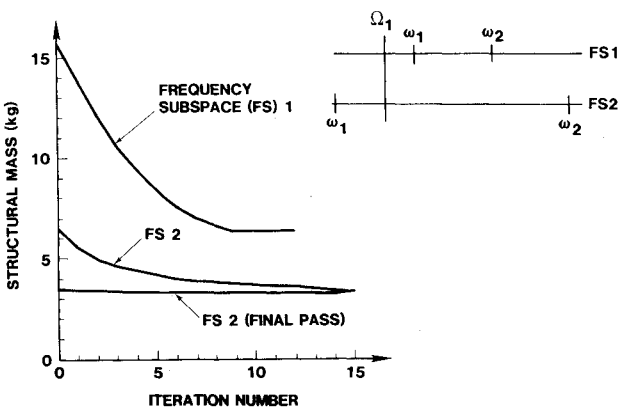

Fig. 7 Two degree of freedom shaft mass history (example 1).

siders a reduced constraint set, the solution is a type of lower bound on the structural mass in that neighboring frequency subspace. It differs from a true lower bound only because the objective function is not the structural mass, but rather the padding parameter η, so that for $\eta^* > 0$ the stage II final design is near the center of the new frequency subspace. If the stage II solution does not successfully generate a feasible lower bound solution with less mass than the current upper bound mass, the trial subspace is deleted from consideration.

The stage III problem provides a convenient test that determines whether the displacement constraint may be reintroduced while maintaining feasibility. When stage III converges with $\eta^* > 0$, a feasible starting design (in the new frequency subspace) is made available for the next stage I problem. It is interesting to note that the stage III problem effectively minimizes the response of the structure (with respect to B dynamic displacement constraints) within the new frequency subspace while retaining an upper limit on the structural mass.

IV. Numerical Examples

A more detailed description of the method reported here as well as an extensive body of computational experience is reported in Ref. 17. In this section numerical results for two examples are selected from Ref. 17 for presentation. The numerical techniques employed include subspace iteration[18] for the eigenanalysis (SADM45 code written by Vanderplaats[20]) and Nelson's method for calculating eigenvector derivatives.[19] The optimum for each stage I, II, or III problem is obtained by solving a sequence of approximate problems using the CONMIN optimizer.[20] All computations were performed on the IBM 3033 computer at UCLA.

All examples are modeled using a six-degree of freedom beam element. The finite element analysis is written for planar grillages in the x-z plane, allowing nodal deflections in the y direction and nodal rotations about the x and z axes. The design of the doubly symmetric thin-walled cross section of Fig. 5a is completely specified by the four cross-section dimensions B, H, t_h, and t_b.

Two Degree of Freedom Shaft (Example 1)

The two degree of freedom shaft of Fig. 5b is selected as the first example. Table 1 contains the input data for this problem and shows that uniformly distributed torsional loading is applied, while rotation constraints are specified at both the end and the midpoint. The cross-section design variables are linked so that only two design variables are independent. Note (Table 1) that damping is included.

Since only two design variables are independent, a mapping of the design space is generated and shown in Fig. 6. It is seen that this map is similar to Johnson's map (Fig. 1), differing mainly in that the feasible region of Fig. 6 is nonconvex while that of Fig. 1 is disjoint. This difference can be attributed to the presence of structural damping ($g = 0.01$) in this example while Johnson's problem was undamped. Note that the dotted line in both Figs. 1 and 6 represents a locus of designs that are characterized by a resonance condition between the first natural frequency and the single forcing function frequency.

The initial analysis of this structure shows that both natural frequencies ($\omega = 554$ Hz, 1930 Hz) are greater than the single loading frequency ($\Omega = 525$ Hz) and the structural mass is 15.8 kg. Optimization in the first frequency subspace reduces the structural mass to 6.41 kg with an active rotation constraint at the tip (node 3). Figure 6 shows the design path in design space while Fig. 7 shows the mass history and the frequency number lines. Table 2 lists the values of the cross-section dimensions and the structural mass while Table 3 shows the natural frequencies.

After finding a candidate optimum in the original frequency subspace, the stage II and III problems [see Fig. 3 and Eqs. (20) and (21)] find a starting design in a different subspace (see Fig. 6). This design is improved by the stage I problem [Eq. (15)] to produce a structural mass of 3.34 kg—a 48% reduction in mass from the first optimum. It can be seen from the mapping of Fig. 6 that the global optimum has indeed been found. Additional attempts to find a better subspace via the stage II and III problems fail, and the process terminates in the second subspace with the node 2 rotation constraint active (see Fig. 5b). This final design is detailed in Table 2 and the mass history is plotted in Fig. 7. Solution time for this problem is 9.8 s.

It is interesting to contrast the two subspace optima listed in Table 2. The subspace 1 optimum is an intuitively satisfying design, featuring a heavier element at the single support, and a lighter element outboard. The subspace 2 design incorporates a distinctly different concept. Here a light, flexible support element is joined to a much heavier outboard element. The design is seen to be a vibration damper type of solution to the problem. This alternative design concept is familiar to most designers, and it is particularly interesting to note that a superior design concept was found via an automated design capability.

Table 1 Input data (example 1)

Material properties:	$E = 2.1 \times 10^{10}$ N/m^2, $\nu = 0.3$, $\rho = 1.1$ kg/m^3
Structural damping:	$g = 0.01$
Element lengths:	$L_1 = 20$ m, $L_2 = 20$ m
Loading:	$T(x) = (1.0 \times 10^4$ Nm/m) sin(525 $H_z t$)
Dynamic constraints:	$\theta_{x2} \leq 0.073$ rad, $\theta_{x3} \leq 0.103$ rad
CSD variable linking:	$B = H = 10t_h = 10t_b$

Side constraints

Variable	Lower bound, m	Upper bound, m
B	0.05	10
H	0.05	10
t_h	0.005	1.0
t_b	0.005	1.0

Table 2 Cross-section dimension history (example 1)

Design element	Variable	Initial design, m	Subspace optimal designs, m: 1	2
1	B	1.0	0.742	0.0524
	H	1.0	0.742	0.0524
	t_h	0.1	0.0742	0.00524
	t_b	0.1	0.0742	0.00524
2	B	1.0	0.509	0.647
	H	1.0	0.509	0.647
	t_h	0.1	0.0509	0.0647
	t_b	0.1	0.0509	0.0647
Active behavior constraints		None	θ_{x3}	θ_{x2}
Structural mass, kg		15.8	6.41	3.34

Table 3 Natural frequency (ω) history (example 1)

Mode	Initial design, Hz	Subspace optimal designs, Hz: 1	2
1	554	819	4.52
2	1930	1600	2380

NB: Load frequency = 525 Hz.

30 Degree of Freedom Delta Wing (Example 2)

The 30 degree of freedom idealized model of a delta wing (see Fig. 8) is studied as the second example. Nonstructural mass has been added as shown in Table 4 to model fuel mass. A two-frequency uniform loading is applied and an envelope of displacement constraints is specified. The 20 design and analysis elements have fixed outside dimensions (B and H) with the height H differing from element to element reflecting the thickness distribution of the wing. An initial analysis shows that the displacements can be modeled with a reduced number of modes, so only 15 modes are included in the subsequent optimization.

The optimization process moves the natural frequencies past the two load frequencies in an orderly progression, eventually exploring nine frequency subspaces with three dynamic behavior constraints critical at the optimum in subspace 9 (see Table 5 and Fig. 9). (For brevity, the table of design variable changes has been omitted here. This information is available in Refs. 17 and 21.) In this problem, several natural frequencies slightly violate the frequency subspace bounds at intermediate subspace optima and are marked with asterisks in Table 5 and Fig. 9. A sample calculation confirms that the frequencies that violate the subspace bounds have mode shapes that are orthogonal to the load distribution for that frequency. The computer run for this example did not terminate after completion of an exhaustive search of all neighboring frequency subspaces, but was stopped in order to conserve computer resources. However, the subspaces early in the $-\nabla\tilde{M}$ ordered list (see Fig. 4) had been explored and rejected so that a restart of the program to complete an exhaustive search is deemed unnecessary. It is interesting to note that an estimated 25% of the total computational effort is spent on the incomplete subspace search performed after an optimum is found in subspace 9. The improvement in structural mass from the subspace 1 optimum (11,100 kg) to the subspace 9 optimum (1730 kg) shows that an 84% reduction is achieved. Solution time for this problem is 1153 s.

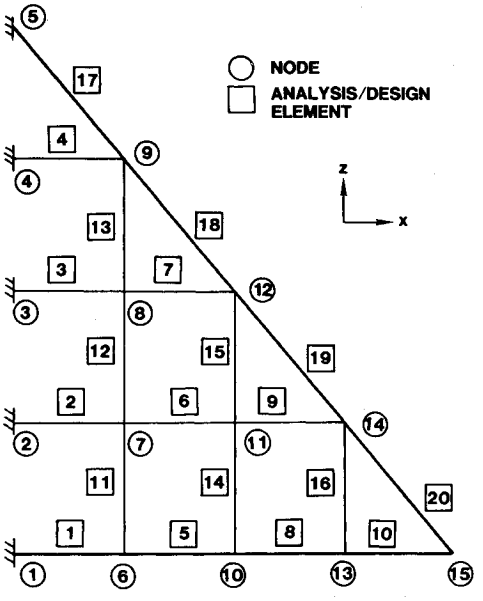

Fig. 8 30 degree of freedom delta wing (example 2).

Table 4 Input data (example 2)

Material properties:	$E = 1.13 \times 10^{11}$ N/m^2 $\nu = 0.3$, $\rho = 4.43 \times 10^3$ kg/m^3
Structural damping:	$g = 0.0$
Element lengths:	$L_1, \ldots, L_{10} = 5$ m $L_{11}, \ldots, L_{16} = 6$ m $L_{17}, \ldots, L_{20} = 7.81$ m
Nonstructural mass, kg node	6: 3270, 7: 7950; 8: 8154 9: 3826, 10: 3131, 11: 6397 12: 3642, 13: 2861, 14: 3249
Loading (nodes 6–15):	$F_y = 1.257 \times 10^5$ N sin(2 Hz t) $+1.257 \times 10^5$ N sin(4 Hz t)
Dynamic constraints:	$U_{y6}, \ldots, U_{y9} \le 0.25$ m $U_{y10}, U_{y11}, U_{y12} \le 0.5$ m $U_{y13}, U_{y14} \le 0.75$ m, $U_{y15} \le 1.0$ m
CSD variable linking:	B, H = constant

	Side constraints	
Variable	Lower bound, m	Upper bound, m
t_h	5.08×10^{-4}	0.02
t_b	4.76×10^{-4}	0.1

Table 5 Natural frequency (ω) history (example 2)

Mode	Initial design, Hz	Subspace optimal design, Hz				
		1	2	7	8	9
1	1.07	0.919	0.650	0.440	0.334	0.329
2	3.40	2.29	1.999*	1.11	0.993	0.986
3	4.14	3.995*	2.93	1.63	1.45	1.43
4	7.39	4.75	4.29	2.44	2.31	2.29
5	8.38	6.90	5.44	2.88	2.64	2.64
6	11.0	7.59	6.12	3.71	3.20	3.13
7	13.5	8.05	6.28	4.20	3.45	3.41
8	14.1	9.76	8.13	4.45	4.13	3.995
9	19.0	10.4	8.68	6.37	5.23	5.20
10	24.0	14.8	10.2	7.59	7.27	7.02
11	27.9	36.1	35.2	32.9	33.4	33.3
12	38.0	47.6	47.7	49.2	49.6	48.9
13	44.5	51.8	51.9	55.2	55.1	55.8
14	51.9	58.0	60.9	49.5	63.9	63.4
15	55.4	70.2	69.8	70.2	71.1	69.9
Active behavior constraints	None	None	None	U_{y6}, U_{y9} U_{y10}, U_{y15}	U_{y8}, U_{y9} U_{y15}	U_{y8}, U_{y9} U_{y15}
Structural mass, kg	67,100	11,100	6,380	2,000	1,730	1,730
Total mass, kg	110,000	53,500	48,900	44,500	44,200	44,200

NB: Load frequencies = 2 HZ and 4Hz.
*Subspace defining frequency constraint is violated.

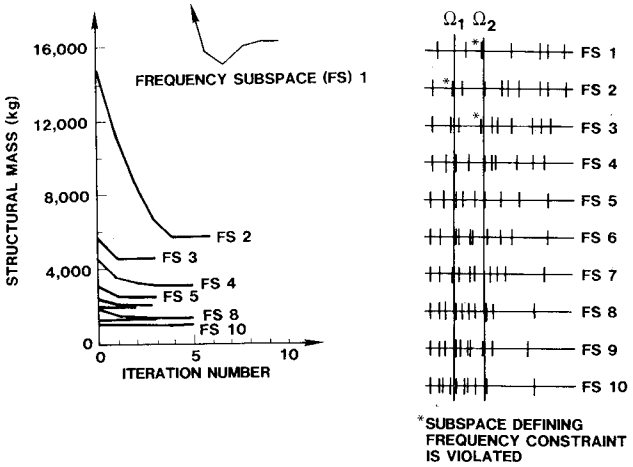

Fig. 9 30 degree of freedom wing mass history (example 2).

V. Conclusions

Examination of frequency subspaces (other than the subspace containing the initial design) has proved extremely profitable. The two numerical examples show that a dramatic reduction in structural mass below the lowest attainable by current techniques is realized for these problems. An innovative approach has been proposed, implemented, and tested which explores a subset of the large number of frequency subspaces. This procedure is not limited in any way to a particular class of structures or analysis techniques, but requires only that the loading be periodic (even the use of the U_{mad} dynamic constraint simplification is not required by the disjoint design space search strategy).

The steepest descent direction $(-\nabla\tilde{M})$ is found to be an effective criterion for frequency subspace ordering. Computational experience indicates that when the result of a stage I optimization can be improved by a shift to a different frequency subspace, that shift usually occurs early in the $-\nabla\tilde{M}$ ordered list.

Supplementary calculations were performed for two examples involving natural frequencies that are nearly resonant with a load frequency. These calculations show that the mode shape is nearly orthogonal to the load distribution for the nearly resonant frequencies. It is likely that the functional dependence of the U_{mad} constraint upon the eigenvectors facilitates designs that exhibit near orthogonality between the load distribution and some eigenvectors. When near orthogonality occurs, the U_{mad} constraint is satisfied even as the design approaches a boundary of the frequency subspace. Thus it is seen that the U_{mad} constraint can be satisfied by modifying the design so as to change the mode shapes as well as the natural frequencies.

The nonlinear form of the U_{mad} constraint, Eq. (14), has proved to be a high-quality explicit approximation when implemented as a nonlinear function formed by introducing linearized eigenvalues and eigenvectors. This form retains the inherent response peak of resonant designs and is limited in accuracy only by the quality of the eigenvalue and eigenvector approximations. It is also worth noting that if the load involves only a single frequency, the worst-case assumption in the U_{mad} formulation is exact.

In summary, it can be said that 1) an innovative approach for dealing with dynamic response constraints has been set forth, implemented, and tested numerically in the context of beam grillage structural systems; 2) a substantial body of computational experience has been gained and it supports the effectiveness of the method; and 3) the basic approach presented can be extended to the general class of damped linearly elastic structures.

Acknowledgment

This research was supported by NASA Research Grant NSG 1490.

References

[1] Cassis, J.H., "Optimum Design of Structures Subjected to Dynamic Loads," UCLA School of Engineering and Applied Science, Los Angeles, Calif., UCLA-ENG-7451, June 1974.

[2] Johnson, E.H., "Disjoint Design Spaces in the Optimization of Harmonically Excited Structures," *AIAA Journal*, Vol. 14, Feb. 1976, pp. 259-261.

[3] Cheng, F.Y. and Srifuengfung, D., "Optimum Structural Design for Simultaneous Multicomponent Static and Dynamic Inputs," *International Journal for Numerical Methods in Engineering*, Vol. 13, 1978, pp. 353-371.

[4] Feng, T.T., Arora, J.S., and Haug, E.J., "Optimum Structural Design under Dynamic Loads," *International Journal for Numerical Methods in Engineering*, Vol. 11, 1977, pp. 39-52.

[5] Haug, E.J. and Feng, T.T., "Optimal Design of Dynamically Loaded Continuous Structures," *International Journal for Numerical Methods in Engineering*, Vol. 12, 1978, pp. 299-317.

[6] Huang, H.C., "Minimum Weight Design of Vibrating Elastic Structures with Dynamic Deflection Constraint," *Transaction of the American Society of Mechanical Engineers, Journal of Applied Mechanics*, March 1976, pp. 178-180.

[7] Icerman, L.J., "Optimal Structural Design for Given Dynamic Deflection," *International Journal of Solids and Structures*, Vol. 5, Pt. 1, 1969, pp. 473-490.

[8] Johnson, E.H., Rizzi, P., Ashley, H., and Segenreich, S.A., "Optimization of Continuous One-Dimensional Structures under Steady Harmonic Excitation," *AIAA Journal*, Vol. 14, Dec. 1976, pp. 1690-1698.

[9] Mroz, Z., "Optimal Design of Elastic Structures Subjected to Dynamic, Harmonically-Varying Loads," *Zeitschrift fur Angewande Mathematik und Mechanik*, Vol. 50, 1970, pp. 303-309.

[10] Pierson, B.L., "A Survey of Optimal Structural Design under Dynamic Constraints," *International Journal for Numerical Methods in Engineering*, Vol. 4, 1972, pp. 491-499.

[11] Plaut, R.H., "Optimal Structural Design for Given Deflection under Periodic Loading," *Quarterly of Applied Mathematics*, Vol. 29, July 1971, pp. 315-318.

[12] Rao, S.S., "Optimum Design of Structures under Shock and Vibration," *Shock and Vibration Digest*, Vol. 7, Dec. 1975, pp. 61-70.

[13] Schmit, L.A. and Miura, H., "Approximation Concepts for Efficient Structural Synthesis," NASA Contractor Rept. 2552, March 1976.

[14] Fleury, C. and Schmit, L.A., "ACCESS 3—Approximation Concepts Code for Efficient Structural Synthesis—User's Guide," NASA Contractor Rept. 159260. Sept. 1980.

[15] Fleury, C. and Schmit, L.A., "Dual Methods and Approximation Concepts in Structural Synthesis," NASA Contractor Rept. 3226, Dec. 1980.

[16] Sheu, C.Y. and Schmit, L.A., "Minimum Weight Design of Elastic Redundant Trusses under Multiple Static Loading Conditions," *AIAA Journal*, Vol. 10, Feb. 1972, pp. 155-162.

[17] Mills-Curran, W.C., "Optimization of Structures Subjected to Periodic Loads," PhD Dissertation, University of California, Los Angeles, 1983.

[18] Dong, S.B., Wolf, J.A. Jr., and Peterson, F.E., "On a Direct Iterative Eigensolution Technique," *International Journal for Numerical Methods in Engineering*, Vol. 14, 1972, pp. 155-161.

[19] Nelson, R.B., "Simplified Calculation of Eigenvector Derivatives," *AIAA Journal*, Vol. 14, Sept. 1976, pp. 1201-1205.

[20] Vanderplaats, G.N., "CONMIN-A Fortran Program for Constrained Function Minimization—User's Manual," NASA TMX 62 282, Aug. 1973.

[21] Mills-Curran, W.C. and Schmit, L.A., "Structural Optimization with Dynamic Behavior Constraints," *Proceedings of the 24th AIAA/ASME/ASCE/AHS Structural Dynamics and Materials Conference*, Pt. 1, May 1983, pp. 369-382.